ON THE EFFECTIVE DOSE ESTIMATION BASED ON TWO-DOSIMETER ALGORITHM: A METHOD TO REDUCE UNCERTAINTY

K. KARIMI SHAHRI[1*], L. RAFAT MOTAVALLI[2], H. MIRI HAKIMABAD[2]

[1] University of Birjand, Physics Department, Faculty of Sciences, Birjand, 9717851367, Iran
[2] Ferdowsi University of Mashhad, Physics Department, Faculty of Sciences, Mashhad, 91775-1436, Iran
[*]*Corresponding author e-mail*: k.karimi@birjand.ac.ir

Received March 19, 2020

Abstract. The *two-dosimeter algorithm* (TDA) is an improved method for estimating the *effective* dose (E) in unknown radiation fields. For such fields, energy spectrum and radiation geometry are not known, although the radiation source characteristics are specified. The two-dosimeter algorithm can be used to overcome these limitations, however, resulting in significant dose overestimations for *Laterals* (LATs), *Overhead* (OH) and *Underfoot* (UF) beam directions. This study attempts to design a *Thermoluminescent Dosimeter* (TLD)-based tool that does not overestimate E for the mentioned radiation directions, by putting a shield on the dosimeter. The shape, materials, and size of the shield were appropriately selected so that the response of the dosimeters was similar to the body when it is irradiated to the external exposure. The shape of the shield was chosen as a half ellipsoid positioned on top of a cylinder with an elliptical surface with appropriate sizes. Aluminum oxide (Al_2O_3) and Chrysoberyl ($BeAl_2O_4$) were considered as materials for the shield. Dosimeters responses have been tested for 0.08, 0.3, and 1 MeV photon energies with various beam directions. Results showed that, by applying these new dosimeters, the two-dosimeter algorithms $E_{est} = 0.97\ R_f + 0.42\ R_b$ and $E_{est} = 0.51\ R_f + 0.22\ R_b$ were obtained for dosimeters with Al_2O_3 and $BeAl_2O_4$ shields, respectively. Using this novel approach, more than 80% of E_{est} was in the –10% to 100% span that is an ideal range of TDA for all photon energies and beam directions. There were overestimations in the order of 200% to 280%, for few irradiation angles, which is much less than the overestimation of the previous algorithm and dosimeters without shield (580%).

Key words: Two-Dosimeter Algorithm, Effective Dose, Dose Estimation Uncertainty, Monte Carlo Simulation.

1. INTRODUCTION

The *effective* dose (E) is recommended by the *International Commission on Radiological Protection* (ICRP) [1] as the basic quantity in radiation protection for radiological protection purposes. This quantity is not measurable, but it can be estimated by an appropriate method. Estimating the radiation risk is usually performed by monitoring the individual personal dosimeters, mounted on the human body [2].

In this case, the estimated E is useful only when a personal dosimeter is directly exposed to the radiation [3]. However, such a limitation may be eased by employing two dosimeters that are exposed simultaneously in the unknown radiation field. Many researchers have sought a useful combination of the response of dosimeters, which are positioned on the front and back of the human body. This is called a *Two Dosimeter Algorithm* (TDA) which will appropriately estimate E for nearly all the conditions encountered during irradiation [4–6]. Indeed, getting access to how E changes into the human body by personal dose monitoring is the motivation for developing the TDA method. According to the best of our knowledge, there is no ideal TDA that can accurately assess E for all irradiation conditions, including different geometries and photon energies. Therefore, an optimal algorithm has been defined to estimate E within –10% to 100% of the real value for most of the incident directions of broad parallel photon beams [7] with range of energies in nuclear power plants (0.08, 0.30, and 1 MeV).

The results of the TDAs, when compared to those of one-dosimeter algorithms, show that the problem of the underestimation when the dosimeter is indirectly irradiated (beam from the back) can be completely solved by placing another dosimeter on the back of the body. Moreover, it has been reported that all the developed algorithms show overestimation in *Laterals, Overhead, and Underfoot geometries* (LOU geometries). This erroneously results in a dramatic reduction of the allowed working time of workers exposed to radiation. The value of E decreases by changing the direction of the incident beam from *anterior-posterior* (AP) to LOU, since the main organs that account for the largest weights in the estimation of E are directly irradiated in AP, whereas these organs are shielded by thick layers of muscle, fat tissues, and also by other organs in LOU geometries. In the same irradiation conditions, not only a reduction of the response of the dosimeters but also a significant increase of response has been observed. This is mainly due to the fact that dosimeters are not shielded similarly to body organs in LOU geometries, and both the front and back dosimeters are underexposed in such geometries. Moreover, the front dosimeter is only irradiated in AP geometry and consequently, dosimeter response and E may show inconsistent results. In order to solve this problem, a dosimeter can be covered by a shielding with an appropriate shape, material, and size, to represent human-body muscle and fat tissues.

It is known that materials with a high atomic number (Z) are mostly used for photon shielding. An appropriate material has been chosen in the present study by considering the dependency of the cross-sections for different radiation interactions such as photoelectric and Compton with photon energy. Aluminum oxide (Al_2O_3) has been suggested as a dosimeter shielding material for estimating the effective dose equivalent (H_E) and effective dose (E) by Han *et al*. [8]. According to their results, the response of a dosimeter shielded with the proposed material is better for predicting H_E and E than a bare one [8]. Dosimeters had been located on an

elliptical phantom which was made from polyethylene and not precisely the real model of the human body.

This study aims to use MCNP Monte Carlo simulations to develop an optimum TDA for estimating E. To this end, dosimeters are located on the ICRP reference adult male voxel phantom (real human model) [9] and covered with different shields. The MCNP Monte Carlo code [10] is used for evaluating E and the response of the dosimeters for hundreds of incident beam directions, according to the definition of E [3, 11] at photon energies of 0.08, 0.3, and 1 MeV. Then, an optimal algorithm is obtained using a systematic analysis of E and dosimeter response data. To evaluate the performance of the proposed method, the results were also compared with those obtained for the previous algorithm [6].

2. MATERIALS AND METHODS

2.1. BEAM DIRECTIONS, PHANTOM, AND DOSIMETER

The source is modeled as a disk that emits photons with anisotropic distribution. It is located on a sphere with a radius of 100 cm from the phantom central point. The angular position of the source around the phantom is determined from the polar and azimuthal angles. The polar angle was defined relative to the height of the phantom (*z*-axis) so that 0° and 180° polar angles are the *Overhead* (OH) and *Underfoot* (UF) beam directions, respectively. The step of change of these angles is selected to be 30° (15° and 165° were also considered). The increase in the azimuthal angle started from the phantom front-side in the clockwise direction with steps of 30°; therefore, an AP beam direction would have a polar angle of 90° and an azimuthal angle of 0°. Simulations have been done using the ICRP reference male voxel phantom whose height and weight are 176 cm and 73 kg. Its data array were included 254 × 127 × 222 voxels where the voxel resolution was 2.137 × 2.137 × 8 mm^3 [9]. This phantom holds all the organs and tissues necessary for dosimetric calculations in a radiation protection field. More anatomical information can be found in the literature [12, 13]. Figure 1 (right) shows the sagittal view of the phantom where the dosimeters are positioned on the front and backsides. Two lithium fluoride (LiF) Thermoluminescent Dosimeter (TLD) were located on the phantom on the chest and at 48 cm below the head. One LiF dosimeter has a diameter of 5 mm, based on Han's recommendations [8], and the other of 6 mm. Both LiF dosimeters have 2 mm thickness (h') (see Figure 1 (left)).

Since the kerma approximation (Mode p, F6 tally with unit of $MeVg^{-1}$) is not reliable for estimating the absorbed dose for some organs [14, 15], the electron transport (Mode e p, *F8 tally with unit of MeV) was also considered. Therefore we performed the calculations on some beam directions for both methods. The results for E did not show significant differences between the calculations with and

without electron transport; thereby the kerma approximation was used to derive the doses absorbed by organs and the dosimeter response, to decrease the simulation time. Then, E was obtained from the sum of the weighted absorbed doses ($\sum_T w_T \sum_R w_R D_T$) with a new tissue weighting factor (w_T) derived from the ICRP103 [3], given a radiation weighting factor (w_R) of 1 for all photon energies. The reported values of E and the dosimeter response were normalized to the air-kerma. Three common photon energies of 0.08, 0.3, and 1 MeV are studied [16, 17].

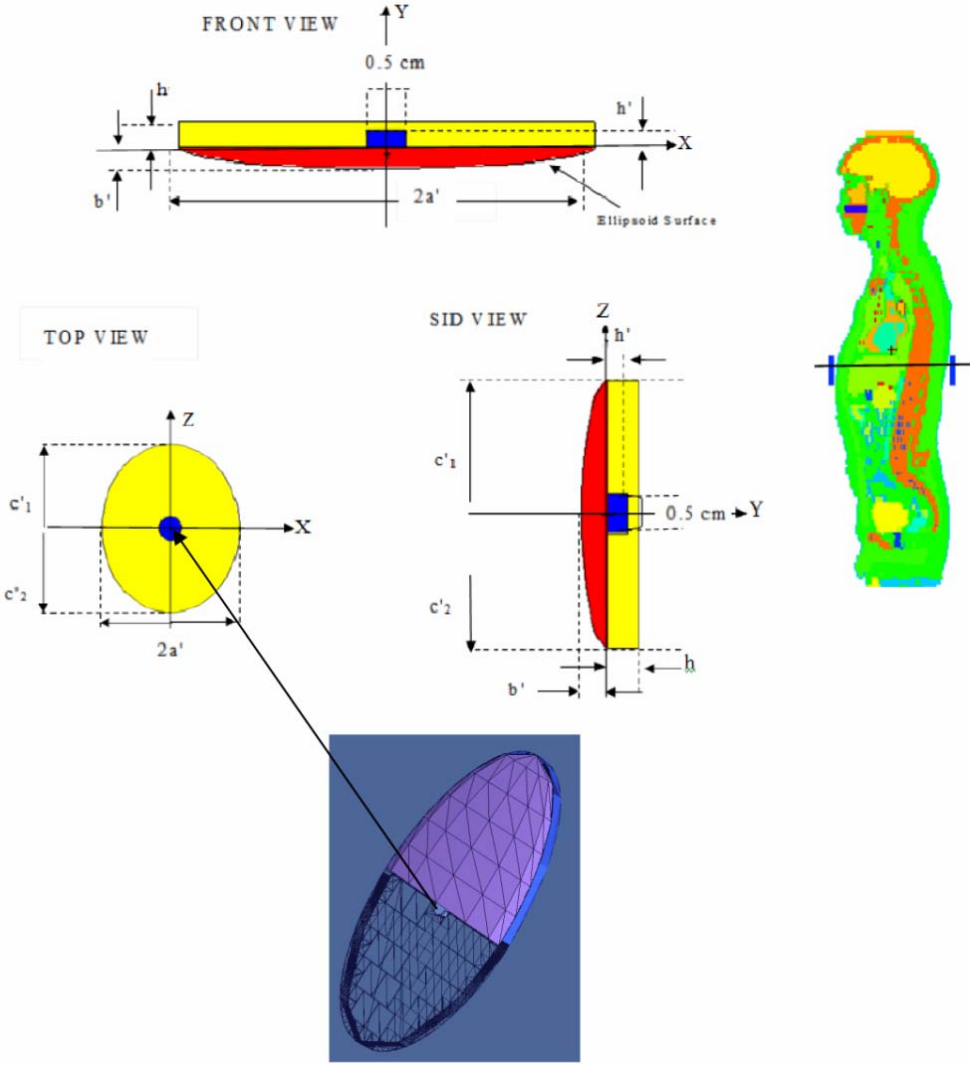

Fig. 1 – Front, side, and top views of the dosimeter with the Al_2O_3 shield. On the right of the Figure, a sagittal view of the ICRP reference phantom illustrates the position of the dosimeters. At the bottom of the figure, a three-dimensional view of the shield displays the dosimeter at its center.

2.2. SHAPE AND MATERIAL OF THE SHIELD

Figure 1 shows the shape of the designed shielding from different views. This study is performed in two distinct steps: first, both major and minor radii of the ellipsoid (a', c') are set to 26 mm and the thickness of the ellipsoid (b') is specified to be 2.62 mm. The height of the cylinder (h) which is positioned under the cut ellipsoid is 3 mm and the size of its elliptical surface is equal to that of the face of the cut ellipsoid. Second, the ellipsoid is cut for the second time with a plane at $z = 0$ and a different value is specified for the minor radius at $z > 0$ and $z < 0$. The physical characteristics of materials used to design dosimeter shielding are shown in Table 1.

Table 1

Properties of the dosimeter shielding materials

Chemical Formula	Density (g/cm^3)	Effective Atomic Number (z_{eff})
Al_2O_3	3.97	10.00
BeO	3.01	6.00
B_4C	2.52	5.15
Na_2CO_3	2.53	8.84
$BeAl_2O_4$	3.79	9.80

For the preliminary calculations, dosimeters are placed on a cylindrical phantom with an elliptical base which was made from a soft tissue. The dimensions of this phantom are based on the dimensions of the trunk of the ICRP phantom. The front and back of the elliptical cylinder phantom are symmetric, therefore it is reasonable to implement only one dosimeter, considering the same response on the front and back dosimeters.

2.3. TWO-DOSIMETER ALGORITHM

To define the TDA, firstly, optimal weighting factors for each dosimeter (w) were obtained by the following procedure. The estimated dose E_{est} is calculated as

$$E_{est} = w\, R_f + (1 - w)\, R_b, \tag{1}$$

where w is assigned different values from 0 to 1 (in steps of 0.1) and E_{est} is calculated for all irradiation geometries. The ratio of E_{est}/E, called r, is calculated for each beam direction. After a comparison between different r values, the maximum (r_{max}) and minimum (r_{min}) and the ratio of r_{max}/r_{min} are determined for a specific w. The optimal w is a value for which r_{max}/r_{min} is the lowest [18]. In this case, the least variation of the discrepancies of E_{est} from E is observed. Considering

the optimal w and the responses of the front (R_f) and back (R_b) dosimeters, E_{est} is determined.

In order to control the underestimation of this algorithm, h(E) has been introduced as an adjustable factor. Calculations have been performed using an in-house FORTRAN program, by multiplying the right side of the eq. (1) by this factor. We have studied different parameterizations of the value of h(E). Finally, h(E) has been determined so that less than 5% of the data have an underestimation.

3. RESULTS AND DISCUSSION

For the calculations, 2×10^8 particles have been tracked to decrease the statistical uncertainty to less than 3% for the scoring tally. For the simulations, 351 input files have been run on a PC with the following specifications: CPU type Intel(R) Core(TM) i7 running at 3.07 GHz, 6.00 GB of RAM and Windows7 (64 bit). The first step is to find suitable shield materials, see section 3.1. Then, the optimal dimensions are determined for these suitable shields, see section 3.2. Overestimations which were resulted in LOU radiation directions, with and without the shield on the dosimeters, are discussed in section 3.3. In section 3.4, the results of twelve dosimeters symmetrically located in different body positions are analyzed to find the best ones.

3.1. SHIELDING MATERIAL

Proper material for shielding was selected based on the agreement between the dosimeter response and E when the direction of the radiation was changed from AP to LOU. Simulations were started by placing the dosimeter on an elliptic cylindrical phantom. Then, the dosimeter was covered by different shielding materials including beryllium oxide (BeO), boron carbide (B_4C), aluminum oxide (Al_2O_3), chrysoberyl ($BeAl_2O_4$), lead beryllium aluminum oxide ($PbBeAl_2O_4$) and sodium carbonate (Na_2CO_3). Figure 2a shows changes of the dosimeter response for different covering materials and E *versus* radiation geometries at 0.08, 0.3, and 1 MeV. For clarity, the E values were removed from Figure 2b. The response of the dosimeter, which was covered by BeO, B_4C, and Na_2CO_3, showed a significant increase when the direction of irradiation changed from LAT to OH at 1 MeV, whereas E showed a considerable decrease. The covered dosimeter with the $PbBeAl_2O_4$ shield showed a significant underestimation, especially for energies of 0.08 and 0.3 MeV due to high photon absorption cross-sections for these energies. There was no significant difference between E values and the dosimeter response when the dosimeter was covered with Al_2O_3, and $BeAl_2O_4$. Thereby, Al_2O_3 and $BeAl_2O_4$ were selected as the best efficient candidates for shielding materials.

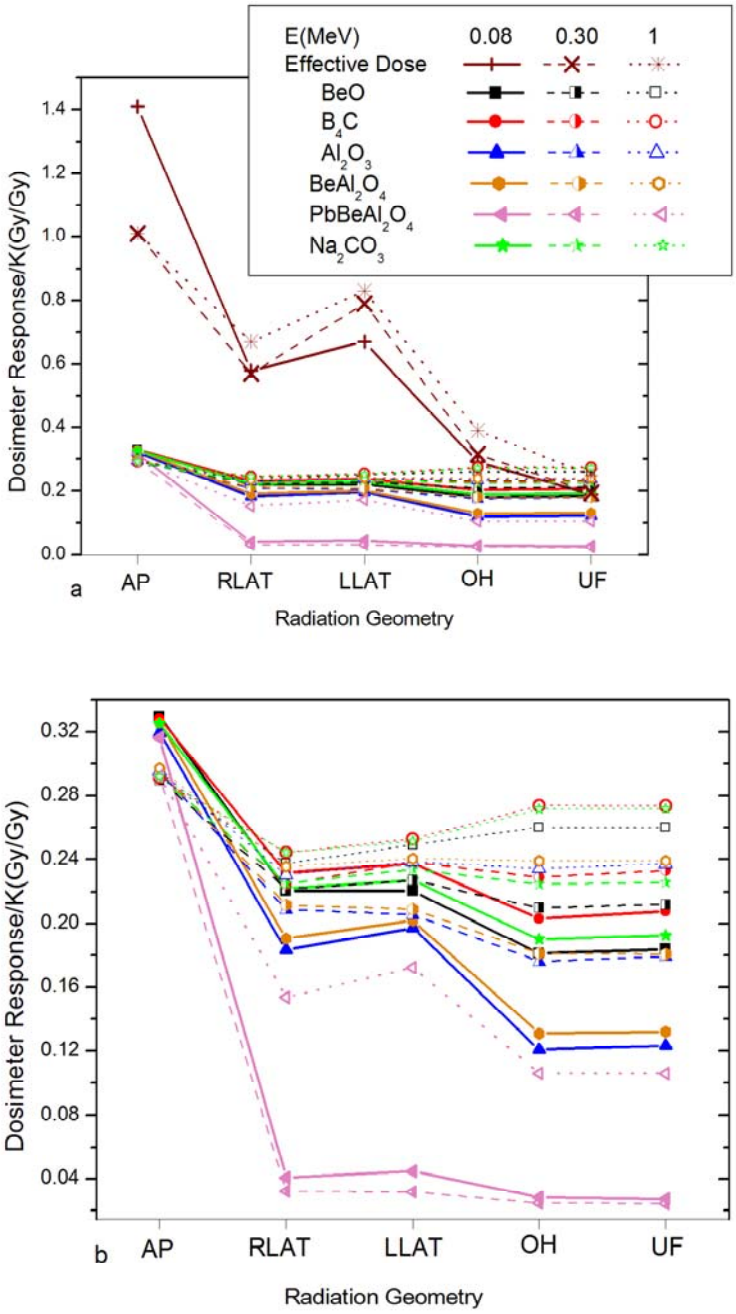

Fig. 2 – The response of the dosimeter for different shielding materials at 0.08, 0.3, and 1 MeV for *anterior-posterior* (AP), *right lateral* (RLAT), *left lateral* (LLAT), *overhead* (OH), and *underfoot* (UF) irradiation geometries. The E is shown in panel a but for clarity it is removed in panel b.

3.2. DETERMINATION OF THE SHIELD SIZE

In this work, firstly, the shield size was selected based on Han's recommendation for Al_2O_3 and $BeAl_2O_4$ with the following values: a' = c' = 26 mm, b' = 2.62 mm and h = 3 mm [8]. In our work, using these suggested sizes, the response of the dosimeter for OH and UF directions was obtained higher than responses for LATs, despite the E changes (Figure 3). Secondly, the ellipsoid minor radius has been cut with the plane at z > 0. Table 2 gives the shield size where c'_1 and c'_2 are the upper and lower minor radii of the simulated ellipsoid, respectively. After changing the ellipsoid minor radius, the variation in the dosimeter response from LATs to OH, or LATs to UF, were similar to E (Figure 4). Derived E_{est} based on the results of the simulations indicated that identified sizes in the 7th case in Table 2 were better than other sizes. The next step was to set the selected shield sizes (a' = 35, b' = 2, c'_1 = 45 and c'_2 = 50 mm) for dosimeters which were positioned on the front and the back of ICRP phantom. $BeAl_2O_4$ were used as shielding material, due to its lower density than Al_2O_3. Moreover, another shield based on Han's recommendation with sizes of a' = c' = 26 mm and b' = 2.62 mm and made of Al_2O_3 was created.

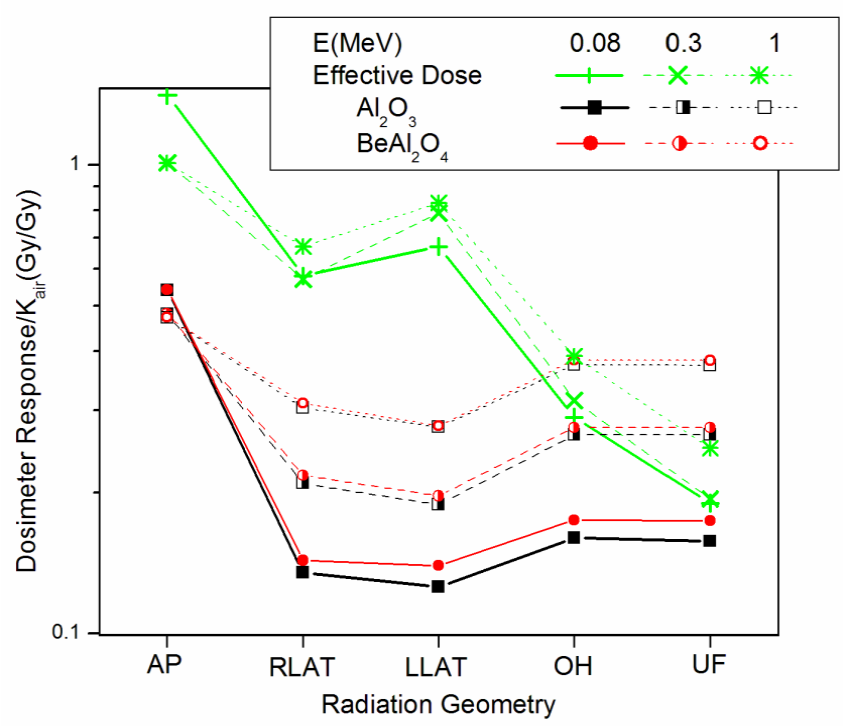

Fig. 3 – Behavior of the dosimeter response for the Al_2O_3 and $BeAl_2O_4$ shields with the dimensions: a' = c' = 26 mm, b' = 2.62 mm and h = 3 mm at 0.08, 0.3, and 1 MeV for AP, RLAT, LLAT, OH, and UF irradiation geometries.

Table 2

Different dimensions of the shields used in this study

case	[1] a' (cm)	[2] b' (cm)	[3] c'_1 (cm)	[4] c'_2 (cm)
1	1.2	0.1	3.0	3.5
2	1.2	0.1	3.5	4.0
3	1.2	0.2	3.0	3.5
4	1.2	0.2	3.5	4.0
5	2.4	0.2	3.5	4.0
6	3.5	0.2	4.0	4.5
7	3.5	0.2	4.5	5

Note: [1] Major radii of ellipsoid; [2] Minor radii of ellipsoid; [3] Minor radii of ellipsoid at $z > 0$; [4] Minor radii of ellipsoid at $z < 0$.

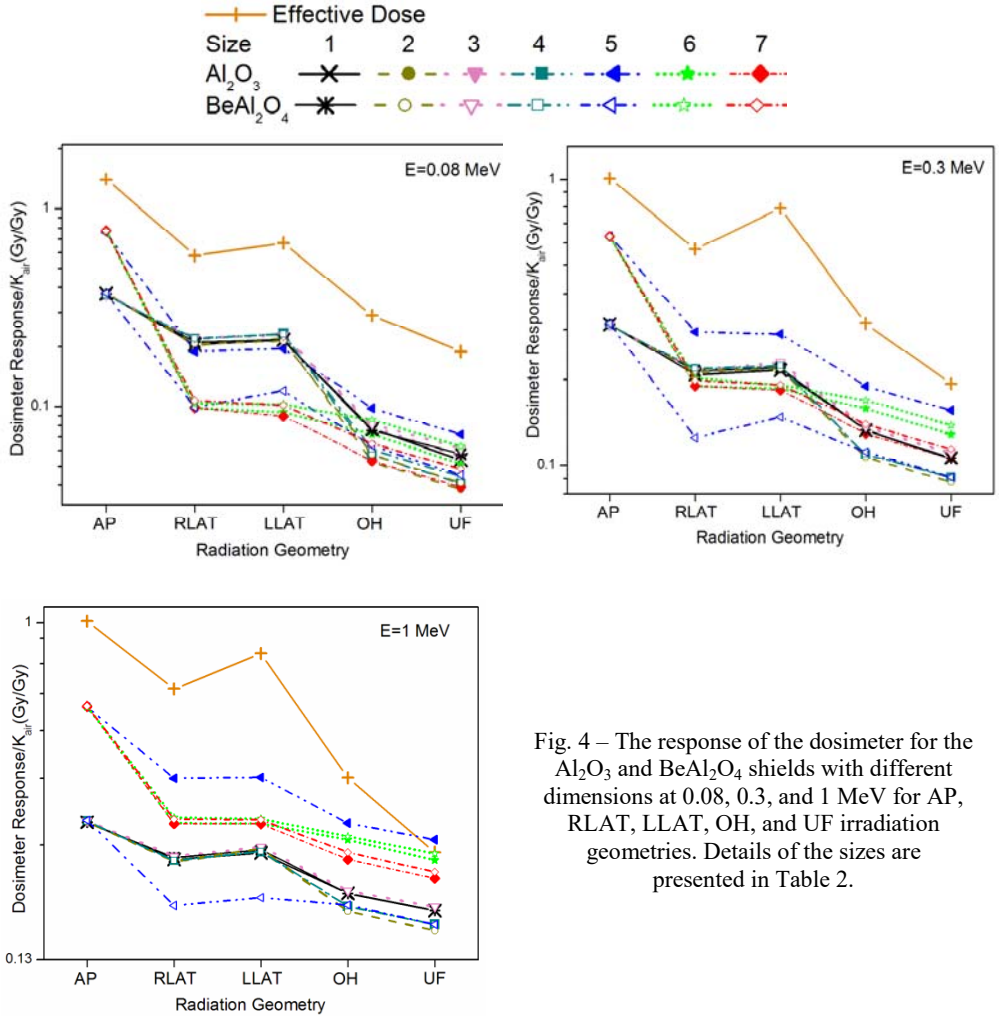

Fig. 4 – The response of the dosimeter for the Al_2O_3 and $BeAl_2O_4$ shields with different dimensions at 0.08, 0.3, and 1 MeV for AP, RLAT, LLAT, OH, and UF irradiation geometries. Details of the sizes are presented in Table 2.

3.3. DETERMINATION OF THE TDA

As mentioned earlier in section 2.3, the optimal weighting factor for each dosimeter should be determined to find an efficient TDA. Figure 5 shows the r_{max}/r_{min} ratio *versus* w when the bare dosimeter (without shield) and the ones covered by $BeAl_2O_4$ and Al_2O_3 shields were positioned on the body.

For bare dosimeters, the ratio of the r_{max}/r_{min} was minimized, when w was set on 0.6. By using the shields on the dosimeters, no minimum value of this ratio was found for a specific w, since nearly the same value was obtained for w = 0.7, w = 0.8, and w = 0.9. h(E) and, therefore, TDA was reported for all the 3 values of w (Table 3).

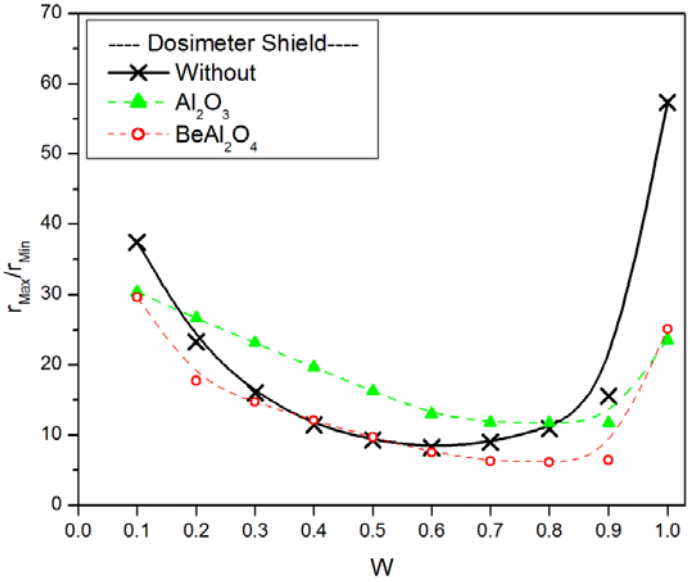

Fig. 5 – Ratios of the maximum and minimum values of E_{est} found by varying the direction of incidence of the beam for different values of w (the weighting factor for the response of the front dosimeter) for a bare dosimeter (without a shield) and the dosimeters with the Al_2O_3 and $BeAl_2O_4$ shields.

Table 3

Values of the adjustable factor (h(E)) and Two Dosimeter Algorithm (TDA) obtained for the bare dosimeter (without shield) and the dosimeter with Al_2O_3 and $BeAl_2O_4$ shields

W	TDA($Sv.Gy^{-1}$)					
	Without shield	h(E)	With Al_2O_3	h(E)	with $BeAl_2O_4$	h(E)
0.60	$E_{est} = 0.74\ R_f + 0.50\ R_b$	1.24	–	–	–	–
0.70	–	–	$E_{est} = 0.97\ R_f + 0.42\ R_b$	1.39	$E_{est} = 0.51\ R_f + 0.22\ R_b$	0.73
0.80	–	–	$E_{est} = 1.37\ R_f + 0.34\ R_b$	1.70	$E_{est} = 0.66\ R_f + 0.16\ R_b$	0.82
0.90	–	–	$E_{est} = 2.14\ R_f + 0.24\ R_b$	2.38	$E_{est} = 1.01\ R_f + 0.11\ R_b$	1.12

The relative difference between E and E_{est} was calculated and tabulated for each case in order to compare the results and to find the optimum TDA (Table 4). In Table 4, the first column represents the ranges of relative differences. The values in each position of the table are the fraction of data (in percent) that fall into different ranges specified in each row. For example, the first number in Table 4 reports, for bare dosimeter, a fraction of 1.43% of the cases in which the difference between E and E_{est} is lower than –10%.

Table 4

Relative difference between E and E_{est} for the bare dosimeter and dosimeters covered by the Al_2O_3 and $BeAl_2O_4$ shields

Relative difference[1]	Without shield	Shield type					
		Al_2O_3			$BeAl_2O_4$		
	W = 0.6	W = 0.7	W = 0.8	W = 0.9	W = 0.7	W = 0.8	W = 0.9
RD ≤ –10%	1.43	2.15	1.79	0.72	2.51	1.43	–
–10 < RD ≤ 0%	12.54	2.51	3.22	4.30	2.51	5.02	5.73
0 < RD ≤ 50%	34.77	58.06	26.52	21.51	45.88	32.97	24.73
50 < RD ≤ 100%	17.57	24.37	35.48	12.19	32.26	29.75	14.35
100 < RD ≤ 200%	18.28	10.03	27.96	29.75	13.62	27.24	27.24
200 < RD ≤ 300%	6.81	2.87	2.87	23.30	3.22	2.51	21.51
300 < RD ≤ 400%	5.02	–	2.15	5.02	–	1.07	4.56
400 < RD ≤ 500%	1.79	–		2.87	–	–	1.47
RD > 500%	1.79	–		0.36	–	–	0.36

An analysis of the results for both $BeAl_2O_4$ and Al_2O_3 shields illustrated that, by increasing w, the percentage of underestimations was decreased, whereas the percentage of overestimation was increased and *vice versa*. Accordingly, the TDAs are given by $E_{est} = 0.51\ R_f + 0.22\ R_b$ and $E_{est} = 0.97\ R_f + 0.42\ R_b$ which were obtained for w = 0.7 with the $BeAl_2O_4$ and Al_2O_3 shields, respectively, results in better agreement than those with w = 0.8 and w = 0.9. Overestimations above 300% were observed for the w = 0.9 results, while the percentage of underestimations of more than 30% was negligible for w = 0.7. Figures 6, 7, and 8 (part a, b and c) show plots of the distributions of the relative difference between E_{est} and E as a function of different polar and azimuthal angles for these two TDAs (parts a and b) and TDA with bare dosimeters (part c) at 0.8, 0.3 and 1 MeV, respectively.

Dosimeter with the Al_2O_3 shield gave better results at 0.08 MeV and the one with the $BeAl_2O_4$ shield revealed the same results at 0.3 and 1 MeV. These findings were the basis for the comparison between results for dosimeters with and without the shields. These comparisons were limited to overestimations for UF, LATs, and OH irradiation geometries that will be described in the following.

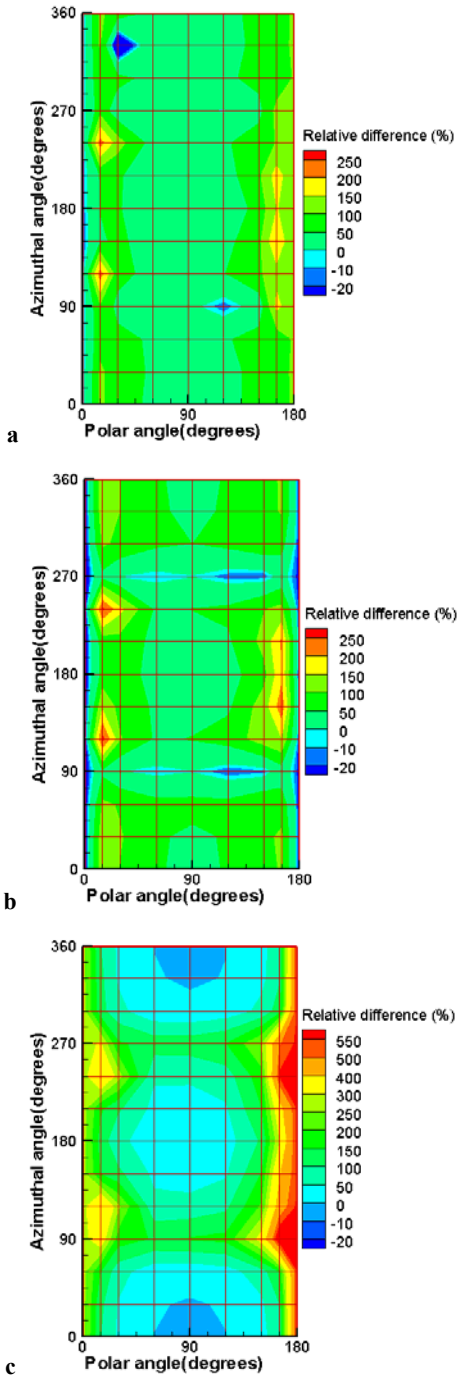

Fig. 6 – Distributions of the relative difference between E_{est} and E with the Al_2O_3 shield (panel a), with the $BeAl_2O_4$ shield (panel b) and with the bare dosimeter (panel c) at 0.08 MeV.

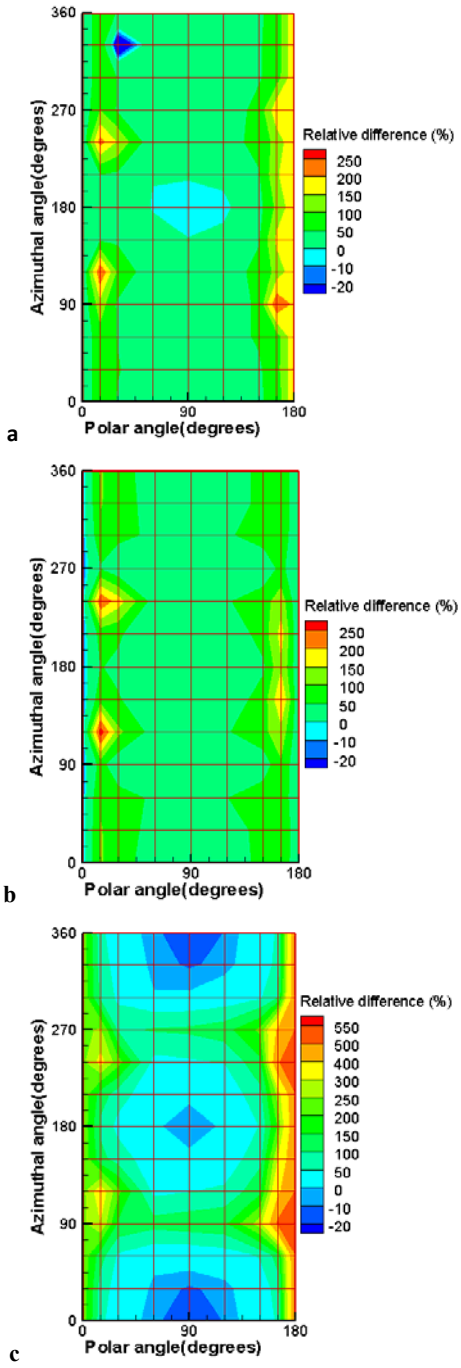

Fig. 7 – Distributions of the relative difference between E_{est} and E with the Al_2O_3 shield (panel a), with the $BeAl_2O_4$ shield (panel b) and with the bare dosimeter (panel c) at 0.3MeV.

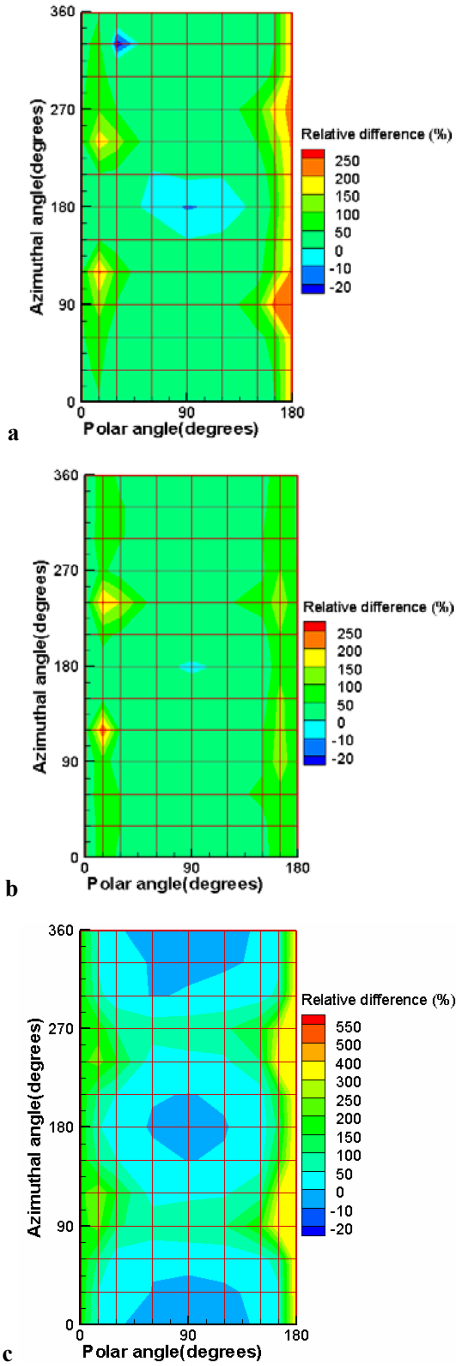

Fig. 8 – Distributions of the relative difference between E_{est} and E with the Al_2O_3 shield (panel a), with the $BeAl_2O_4$ shield (panel b) and with the bare dosimeter (panel c) at 1MeV.

In UF geometry, an overestimation of up to 560% was observed for bare dosimeters whereas this overestimation decreased to a range of 0% to 100% by using the new dosimeters at 0.08 MeV. With the increase of the energy to 0.3 MeV, the overestimation was almost removed and ranged from 0% to 50% at 1 MeV. In LATs geometries, by applying the new TDA, overestimations at 0.08 MeV were completely removed and were limited to 0% to 50% range at 0.3 MeV and 1 MeV. There were two exceptions at $\theta = 15°$ and $\theta = 165°$ where the overestimations reached above 50%. In these radiation directions, sensitive organs and almost all of the abdominal organs received a non-significant dose, thereby the value of E was very small (Figure 6c). Both dosimeters, especially the back dosimeter, were underexposed in such radiation directions, therefore their corresponding E_{est} was greater than E which leads to the overestimation. In OH geometry, overestimations above 200% were changed to an underestimation at 0.08 MeV and 0.3 MeV, and finally, they were reduced to a range of 0% to 50% at 1 MeV using the new dosimeters and TDAs. In this irradiation geometry, photons cannot reach the LiF dosimeters owing to the shielding cover, especially when the person is irradiated from azimuthal angles such as $\varphi = 120°$ and $\varphi = 270°$. If the thickness of their shield would have been made thinner, greater overestimations occurred at the energy of 1 MeV.

Generally, by using the newly designed dosimeters only overestimations of the order of 200% to 280% were seen in a few number of irradiation angles, while the amount of these overestimations reached up to more than 550% with the bare dosimeters.

3.4. POSITIONS OF THE DOSIMETERS

Twelve dosimeters were symmetrically located in different body positions. These positions were included right and left arms, right and left wrists, abdomen and spine, chest and back, neck and nape, right and left neck. TDAs which were acquired from each of the mentioned dosimeter pairs are illustrated in Figure 9.

In this figure, the frequency distribution of the data is plotted versus the relative difference between E and E_{est}. The important point to choose the optimum TDA is the percentage of data that falls in the range of –10% to 100% (Figure 9), presenting more accuracy of the derived data. As can be seen from Figure 9, the capability of the algorithm to estimate E is reduced from bottom to top. Therefore, favorable results were obtained when the dosimeters were positioned on the front and back, due to the fact that sensitive organs with big tissue weighting factors existed in the abdomen.

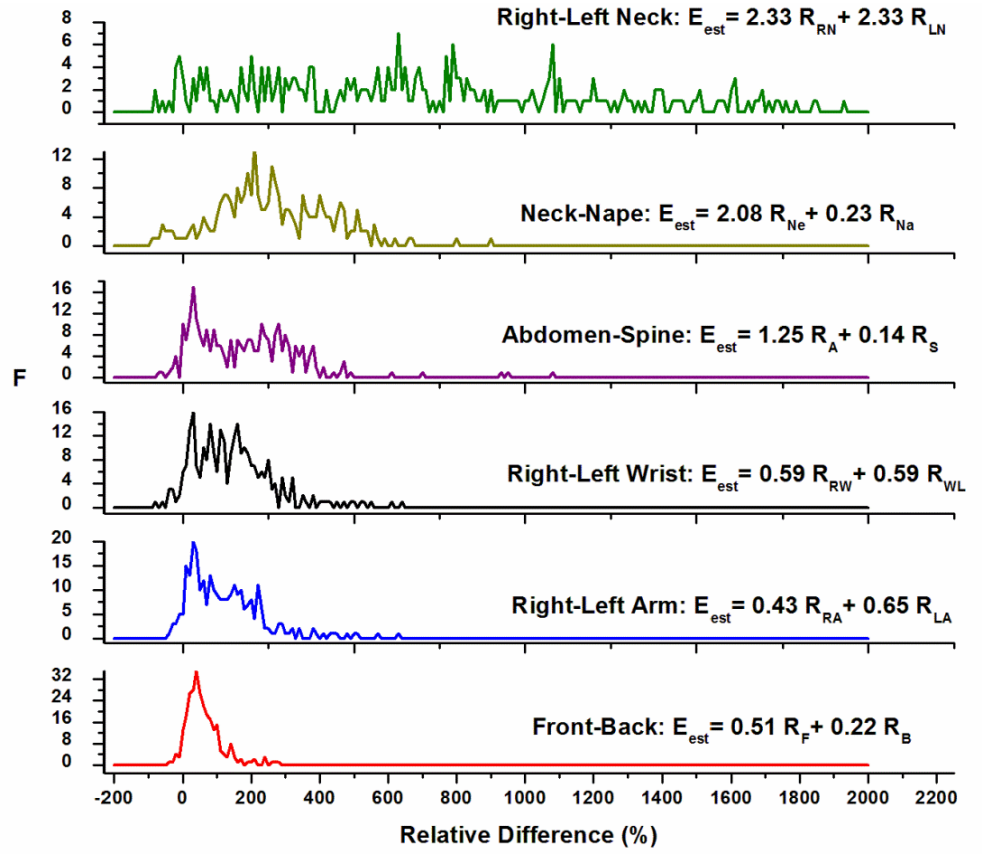

Fig. 9 – Frequency distribution of the relative difference between E and E_{est} for dosimeters placed on the chest and back, on the right and left of the arm, right and left wrist, abdomen and spine, neck and nape and right and left neck from bottom to top, respectively.

4. CONCLUSION

The present study attempts to improve the accuracy of TDA for practical implementations. Results showed that the proposed TDAs may not provide reliable results at $\theta = 15°$ and $\theta = 165°$ where effective dose E is small but E_{est} is large, showing significant overestimations. From our results, it is concluded that, if a person works in an occupational environment where 0.08 MeV energy dominates, a dosimeter with Al_2O_3 shield is more effective. In contrast, the dosimeter with the $BeAl_2O_4$ shield is more suitable in an environment with higher energies. Generally, the $BeAl_2O_4$ shielding should be placed on dosimeters if there are different energies in the occupational environment. However, when the energy is not crucial and the personnel works for many hours, the weight of the dosimeter can be more

important; therefore the dosimeter with the Al_2O_3 shielding is suggested because it weighs 40 g *versus* the 85 g of $BeAl_2O4$. Applying the new TDAs for improving the estimation of E is more important in unknown fields. The results also show that two dosimeters should be placed on the front and back of the body.

Acknowledgements. This study was supported by a grant from the University of Birjand (d/25020-13/11/1395).

REFERENCES

1. International Commission on Radiological Protection ICRP Publication 60: *1991 Recommendations of the International Commission on Radiological Protection*. Ann ICRP 21(1–3). Pergamon Press, Oxford (1991).
2. H.G. Kim and T.Y. Kong, *Application and experience of a two-dosimeter algorithm for better estimation of effective dose during maintenance periods at Korea nuclear power plants*. Appl. Radiat. Isot. **67**(7), 1315–1319 (2009).
3. International Commission on Radiological Protection ICRP Publication 103: *The recommendations of the International Commission on Radiological Protection*. Ann 37(2–4). Elsevier, Amsterdam, (2007).
4. H.G. Claycamp, *Optimization of monitor weighting factors for the estimation of effective dose equivalent from external photon exposures*, Radiat. Prot. Dosim, **63**(2)**,** 105–111 (1996).
5. C.H. Kim, S. Cho, J.H. Jeong, W.E. Bolch, W.D. Reece, and J.W. Poston, *Development of new two-dosimeter algorithm for effective dose in ICRP publication 103*, Health. Phys. **100**(5), 462–467 (2011).
6. K. Karimi-Shahri, L. Rafat-Motavalli, H.Miri-Hakimabad, L. Liu, and J. Li, *Effects of Computational phantoms on the effective dose and two-dosimeter algorithm for external photon beams*, Appl. Radiat. Isot. **115**, 155–164 (2016).
7. National Council on Radiation Protection and Measurements. *Use of Personal Monitors to Estimate Effective Dose Equivalent and Effective Dose to Workers for External Exposure to Low-LET Radiation.* NCRP Report No. 122 (Bethesda, MD: NCRP) (1995).
8. H.J. Han, W.D. Reece, and C.H. Kim, *Improved estimates of effective dose equivalent using two optimal anisotropic responding dosimeters*, Health. Phys. **77** (5), 536–540 (1999).
9. International Commission on Radiological Protection ICRP Publication 110: *Adult Reference Computational Phantoms*. Ann ICRP39 (2). Elsevier, Amsterdam (2008).
10. J.F. Briesmeister, Editor mcnp^{tm} – *a general Monte Carlo N-particle transports code: version 4C*.Report LA-13709-M, Los Alamos National Laboratory Los Alamos. 1–427 (2000).
11. H. Miri H, L. Rafat M, and K. Karimi S, *Different effective dose conversion coefficients for monoenergetic neutron fluence from 10^{-9} MeV to 20 MeV-A methodological comparative study,* Radioprotection **47**(2), 271–248 (2012).
12. International Commission on Radiological Protection ICRP Publication 89: *Basic anatomical and physiological data for use in radiological protection reference values*. Ann ICRP 32(3–4). Pergamon Press, Oxford (2002).
13. A. Ebrahimi Khankook, H. Miri Hakimabad, and L. Rafat Motavalli, *A feasibility study on the use of phantoms with statistical lung masses for determining the uncertainty in the dose absorbed by the lung from broad beams of incident photons and neutrons*. J. Radiat. Res. **58**(3), 313–328 (2017).
14. International Commission on Radiological Protection ICRP Publication 116: *Conversion coefficients for radiological protection quantities for external radiation exposures*. Ann ICRP **40**(2–5). Elsevier, Amsterdam (2010).

15. K. Karimi-Shahri, L. Rafat-Motavalli, and H. Miri-Hakimabad, *Study of size, type and the kerma approximation for thermoluminescent dosimetry*, J. Radioanal. Nucl. Ch. **298**(2), 813–819 (2013).
16. P.L. Roberson, G. W. R. Endres, R. A. Fox, D.L. Haggard, K. L. Holbrook, and L.A. Rathbun, *Spectral and dosimetric measurements of photon fields at commercial nuclear sites*, Report pnl-4915, nureg/cr-3569 (Richland, WA: Pacific Northwest National Laboratory) (1984).
17. W.D. Reece, J.W. Poston, and X.G. Xu, *Assessment of effective dose equivalent for external photon radiation Vol. I: Calculational results for beam and point source geometries,* Radiat. Prot. Dosim. **55**(1), 5–21 (1994).
18. C.H. Kim, W.D. Reece, and J.W. Poston, *Development of a two dosimeter algorithm for better estimation of effective dose equivalent and effective dose*, Radiat. Prot. Dosim. **81**(2), 101–112 (1999).